Mössbauer effect in $R_2Fe_{14}B$ compounds

F. E. Pinkerton
Physics Department, General Motors Research Laboratories, Warren, Michigan 48090-9055
W. R. Dunham
Institute of Science and Technology, University of Michigan, Ann Arbor, Michigan 48109

We report room temperature Mössbauer spectra for $R_2Fe_{14}B$ compounds with R = Y, Ce, Pr, Nd, Gd, Dy and Ho. The hyperfine fields are obtained for the six inequivalent iron sublattices in the $R_2Fe_{14}B$ crystal structure. The internal magnetic fields scale with the Curie temperature, but the spectra are otherwise virtually independent of the rare-earth component. These results indicate that the electronic configurations of the iron atoms are nearly the same for all these compounds, and that the iron 3*d* shell dominates the conduction electron polarization contribution to the internal fields.

Recently developed rare earth-iron-boron alloys using Nd or Pr rival Sm-Co as high performance permanent magnet materials.[1–6] High energy products have been reported for Nd-Fe-B magnets prepared either by rapid solidification[1,2] or by powder metallurgy techniques.[6] The rapidly solidified Nd-Fe-B alloys can develop intrinsic coercivities as large as 20 kOe.[2] X-ray and neutron diffraction studies[7] reveal that the high coercivity materials are comprised principally of the new ternary phase $R_2Fe_{14}B$.

We have previously reported the ^{57}Fe Mössbauer spectrum of $Nd_2Fe_{14}B$,[8] from which we extracted the internal magnetic fields H_N for the iron sublattices. Here we extend this work to a systematic investigation of the $R_2Fe_{14}B$ spectra across the rare-earth (R) series, with R = Y, Ce, Pr, Nd, Gd, Dy, and Ho. We find that the shape of the spectrum is essentially independent of the rare-earth component, implying that the internal fields at the iron nuclei are dominated by the iron 3*d* electrons. Variations in the overall width of the spectra for different R reflect changes in the Curie temperature T_C.

The ^{57}Fe absorbence spectra[9] were measured on single phase powder samples[10] using a 14.4-keV gamma-ray spectrometer. The spectra shown in Figs. 1–3 for R = Pr, Gd, and Ho exemplify the behavior across the rare-earth series. The $Pr_2Fe_{14}B$ spectrum in Fig. 1 is nearly indistinguishable from that previously reported for $Nd_2Fe_{14}B$,[8] and similar spectra are seen for Gd (Fig. 2) and Ho (Fig. 3). The complexity of these spectra stems from the large number of distinct iron sites in the $R_2Fe_{14}B$ crystal structure.

The $R_2Fe_{14}B$ compounds[7] (space group $P4_2/mnm$) have 56 iron atoms per tetragonal unit cell, arranged on six crystallographically inequivalent sites: two *k* sites each with occupation 16; two *j* sites each with occupation 8; and one *c* and one *e* site, each with occupation 4. We can thus decompose the complete Mössbauer spectrum into six iron subspectra with these intensity ratios. We represent the hyperfine interactions at each site by a Hamiltonian, given by Kundig,[11] which includes both internal magnetic field and electric field gradient (EFG) terms. The spectrum of each site is described by six parameters: the isomer shift *IS*; the internal field H_N; the quadrupole interaction $1/2eQV_{zz}$ (where $V_{zz} = \delta^2 V/\delta z^2$ is the major axis component of the EFG tensor), the angles θ and ϕ specifying the direction of the H_N with respect to the EFG; and the asymmetry parameter $\eta = (V_{xx} - V_{yy})/V_{zz}$ of the EFG tensor. We follow the usual convention that the EFG tensor components V_{xx}, V_{yy}, and V_{zz} in its principal axis system are chosen such that $|V_{zz}| \geqslant |V_{yy}| \geqslant |V_{xx}|$, i.e., $0 \leqslant \eta \leqslant 1$. The site parameters are extracted from a computer minimization fit to the total spectrum, with the site intensities constrained to be 16 : 16 : 8 : 8 : 4 : 4. The fitting algorithm, which minimizes the root-mean-square error by quadratic interpolation in Fourier space, is a combination of the computer synthesis technique of Kundig[11] and our fast Fourier transform minimization techniques developed for fitting electron spin resonance data for free radicals.[12]

All the sites in the $R_2Fe_{14}B$ spectra have a relatively

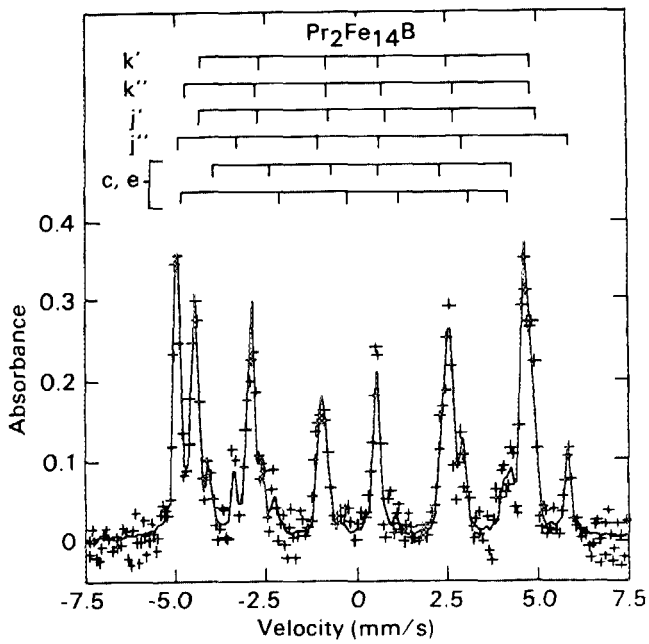

FIG. 1. Room temperature ^{57}Fe Mössbauer spectrum of $Pr_2Fe_{14}B$. The crosses are the experimental data. The solid curve is a six site computer fit as explained in the text, assuming a full width-half maximum (FWHM) linewidth of 0.16 mm/s. The six derived subspectra are indicated above the spectrum, and the extracted Mössbauer parameters are given in Table I.

 0021-8979/85/014121-03$02.40

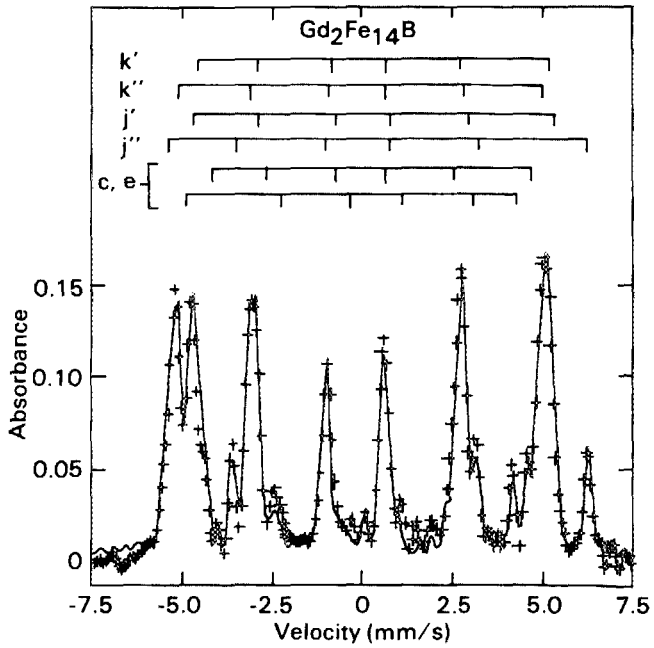

FIG. 2. Room temperature ^{57}Fe Mossbauer spectrum of $Gd_2Fe_{14}B$. The crosses are the experimental data. The solid curve is the computer fit using a FWHM linewidth of 0.17 mm/s, with the parameters given in Table I.

small quadrupole interaction compared to the internal field ($|eQV_{zz}/2g_{3/2}\mu_N H_N|$ ranges from ~ 0 to about 0.4). In this regime the spectrum is only weakly dependent on the angles θ and ϕ, and is nearly independent of the choice of η. Given the complexity of the spectrum, it is not possible to uniquely determine θ, ϕ and η. The fits assume that the EFG is axially symmetric and parallel to H_N ($\theta = \phi = \eta = 0$).[13]

The solid curves in Figs. 1–3 are the computer fits to the observed spectra. The component subspectra are indicated

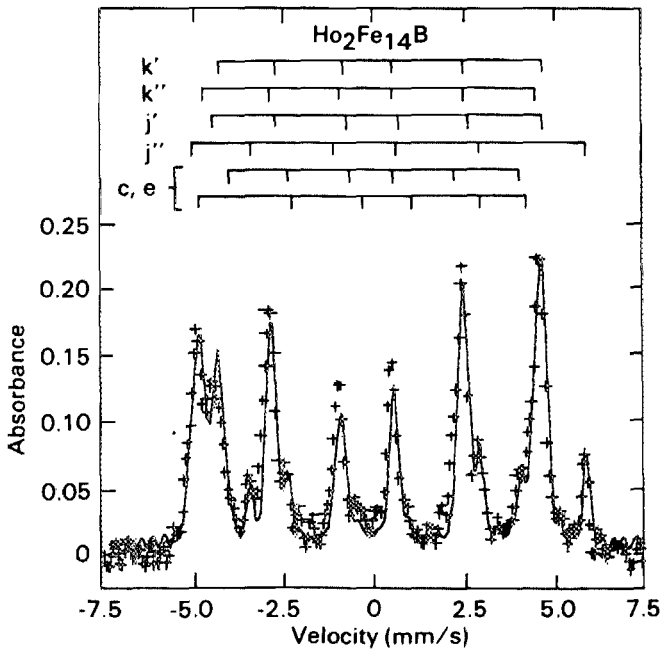

FIG. 3. Room temperature ^{57}Fe Mossbauer spectrum of $Ho_2Fe_{14}B$. The crosses are the experimental data. The solid curve is the computer fit using a FWHM linewidth of 0.17 mm/s, with the parameters given in Table I.

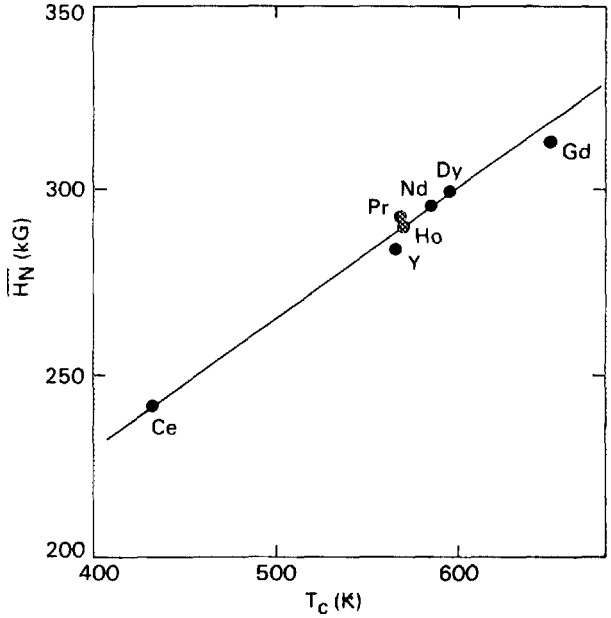

FIG. 4. Average internal magnetic field $\overline{H}_N$ vs the $R_2Fe_{14}B$ Curie temperature T_C. The line is a guide to the eye.

above each spectrum, while the corresponding Mössbauer parameters are given in Table I. The isomer shifts are small (± 0.2 mm/s), indicating that the electronic configurations of the iron atoms are close to that in metallic iron. The internal fields are also comparable to that of metallic iron at room temperature[14] ($H_N = 330$ kG). The two inequivalent k sites give rise to the doublet near -5 mm/s, while the peak at $+6$ mm/s corresponds to the j'' site having both a large internal field and a substantial quadrupole splitting. The c and e sites (which are indistinguishable on the basis of intensity alone) have low intensity (only 7% each of the total intensity); their assignments have the greatest uncertainty.

TABLE I. Isomer shift IS, internal field H_N, and quadrupole interaction $eQV_{zz}/2$ for the six iron sites in $R_2Fe_{14}B$ compounds at room temperature. The site intensities are in the ratio 16 : 16 : 8 : 8 : 4 : 4. The error estimates given in the first row are typical for the entire table.

R	Site	IS (mm/s)	H_N (kG)	$eQV_{zz}/2$ (mm/s)
Pr	k'	-0.03 ± 0.04	282 ± 4	0.36 ± 0.1
	k''	-0.19	295	0.03
	j'	0.04	291	0.28
	j''	0.08	336	0.67
	c,e	-0.03	257	0.24
		-0.06	280	-0.83
Gd	k'	0	303	0.37
	k''	-0.22	314	0.07
	j'	0.05	313	0.23
	j''	0.08	363	0.58
	c,e	-0.08	278	0.28
		-0.11	286	-0.73
Ho	k'	0	279	0.35
	k''	-0.23	288	0.06
	j'	-0.01	287	0.10
	j''	0.07	340	0.63
	c,e	-0.10	249	0.02
		-0.07	282	-0.70

The shape of the $R_2Fe_{14}B$ spectrum is essentially independent of the rare-earth component. This is demonstrated explicitly in Figs. 1–3 but applies as well to $Nd_2Fe_{14}B$ (Ref. 8) and the other rare earths we have studied (R = Y, Ce, Dy). The primary effect of changing R is a scaling of the internal fields, that is, a change in the overall width of the spectrum. The remaining subtle changes are easily accommodated by modest adjustments of the parameters. Evidently the internal fields at the iron sites have little sensitivity to the magnitude or direction[15] of the localized $4f$ moments on the rare earths. Similar behavior characterizes RFe_2 compounds in which the iron $3d$ electrons dominate the conduction electron polarization contribution to H_N.[16]

The internal field scaling with changing R reflects the variation of the Curie temperature T_C among $R_2Fe_{14}B$ compounds. This is seen in Fig. 4, where the average internal field $\bar{H}_N$ is plotted as a function of T_C. As T_C increases, the room temperature internal fields grow, as qualitatively expected for smaller T/T_C. The role of the rare earth is likely the secondary one of modifying T_C through changes in the R-R exchange. The internal fields then respond primarily to the core polarization by the d electron moments.

The average iron internal field in $Y_2Fe_{14}B$ is $\bar{H}_N = 284$ kG. From the measured room temperature saturation moment $M_s = 1100$ G, the average moment per Fe atom is estimated to be $1.92\,\mu_B$. The ratio of $150\ \mathrm{kG}/\mu_B$ is in excellent agreement with the value ($145\ \mathrm{kG}/\mu_B$) obtained from a variety of Y-Fe compounds.[17] The virtual independence of the Mössbauer spectrum on R suggests that this correspondence persists throughout the $R_2Fe_{14}B$ series.

In conclusion, we find that the Mössbauer spectra of $R_2Fe_{14}B$ compounds with R = Y, Ce, Pr, Nd, Gd, Dy, and Ho are nearly independent of the rare earth component. Scaling of the internal fields with changing R are qualitatively explained on the basis of changing Curie temperatures. These observations imply that the $4f$ moments have little influence on H_N at the iron site. The iron configurations are nearly the same in all these compounds, and as in RFe_2 compounds,[16] the conduction electron contribution to H_N is dominated by the iron $3d$ electrons. The spectra are fit well by a six-site Hamiltonian with the relative site intensities constrained to the site occupations obtained from the crystal structure.[7]

ACKNOWLEDGMENTS

We would like to thank C. D. Fuerst, J. F. Herbst, J. J. Croat, R. W. Lee, and J. R. Smith for valuable discussions, and F. E. Jamerson for his enthusiastic support. We are grateful to E. A. Alson for preparing the samples and T. H. Van Steenkiste for technical support.

[1] J. J. Croat, J. F. Herbst, R. W. Lee, and F. E. Pinkerton, Appl. Phys. Lett. **44**, 148 (1984).
[2] J. J. Croat, J. F. Herbst, R. W. Lee, and F. E. Pinkerton, J. Appl. Phys. **55**, 2078 (1984).
[3] N. C. Koon and B. N. Das, J. Appl. Phys. **55**, 2063 (1984).
[4] G. C. Hadjipanayis, R. C. Hazelton, and K. R. Lawless, J. Appl. Phys. **55**, 2073 (1984).
[5] D. J. Sellmyer, A. Ahmed, G. Muench, and G. C. Hadjipanayis, J. Appl. Phys. **55**, 2088 (1984).
[6] M. Sagawa, S. Fujimura, M. Togawa, H. Yamamoto, and Y. Matsuura, J. Appl. Phys. **55**, 2083 (1984).
[7] J. F. Herbst, J. J. Croat, F. E. Pinkerton, and W. B. Yelon, Phys. Rev. B **29**, 4176 (1984).
[8] F. E. Pinkerton and W. R. Dunham, Appl. Phys. Lett. **45**, 1248 (1984).
[9] W. R. Dunham, C. T. Wu, R. M. Polichar, R. H. Sands, and L. J. Harding, Nucl. Instrum. Methods **145**, 537 (1977).
[10] The samples were confirmed to be single phase both by optical metallographic analysis of the starting ingot and by x-ray diffraction on the powder.
[11] W. Kundig, Nucl. Instrum. Methods **48**, 219 (1967).
[12] W. R. Dunham, J. A. Fee, L. J. Harding, and H. J. Grande, J. Magn. Reson. **40**, 351 (1980).
[13] Relaxation of this assumption has a negligible effect on IS and H_N, but can substantially alter the value obtained for the quadrupole interaction $eQV_{zz}/2$.
[14] R. S. Preston, S. S. Hanna, and J. Heberle, Phys. Rev. **128**, 2207 (1962).
[15] The rare-earth and iron moments are parallel in $Nd_2Fe_{14}B$ (Refs. 6 and 8) and the other light rare earths, and are expected to be antiparallel among the heavy rare earths.
[16] G. K. Wertheim and J. H. Wernick, Phys. Rev. **125**, 1937 (1962).
[17] P. C. M. Gubbens, J. H. F. van Apeldoorn, A. M. van der Kraan, and K. H. J. Buschow, J. Phys. F **4**, 921 (1974).